A methodology to compare the performance of material models in the framework of material testing 2.0

Peshave, A.[1a], Pierron F. [2], Lava, P. [2], Moens, D. [1], Vandepitte, D. [1]

[1a]KU Leuven, Celestijnenlaan 300 - box 2420, 3001 Leuven, Belgium, [2]MatchID NV, Leiekaai 25a, 9000 Ghent, Belgium, [a]amar.peshave@kuleuven.be

Abstract: Full field optical measurement techniques such as digital image correlation (DIC) provide a means to measure the information-rich heterogeneous strain states. Material testing 2.0 aims to exploit this by designing mechanical tests aimed at inversely identifying the underlying material properties. Knowledge of material behaviour, which is an important aspect of machine design, might not be available *a priori*. This makes it necessary to fit different material models to the same underlying measurement data and choose one that fits the best. In this work, digital image correlation (DIC) tests are performed on a notched high density polyethylene (HDPE) sample under uniaxial load. Full-field strains thus obtained are used in combination with the virtual fields method (VFM) to identify parameters of 3 different hyperelastic material models. Two metrics are used to compare their performance: equilibrium gap indicator (EGI) and reconstructed axial force ratio (RAFR). It is found that hyperelastic material models do not capture the material behaviour in the small strain regime. To address this, a linear-elastic contribution, exponentially decaying with the equivalent shear stress is added to the hyperelastic material models and parameters are identified using VFM. It is found that the elastic-hyperelastic material models perform better than their purely hyperelastic counterpart.

Introduction: Stereo-DIC tests are performed on a notched high density polyethylene (HDPE) test sample under uniaxial load (refer Figure 1a). The DIC strain fields thus obtained (refer Figure 1b) are used in conjunction with the virtual fields method (VFM) [1] to identify the material parameters of Neo Hookean, 2-parameter Mooney Rivlin and Yeoh material models. DIC dataset used for material identification consists of 47 time steps involving loads and peak axial strains in the range of 0-1000N and 0-8.7% respectively.

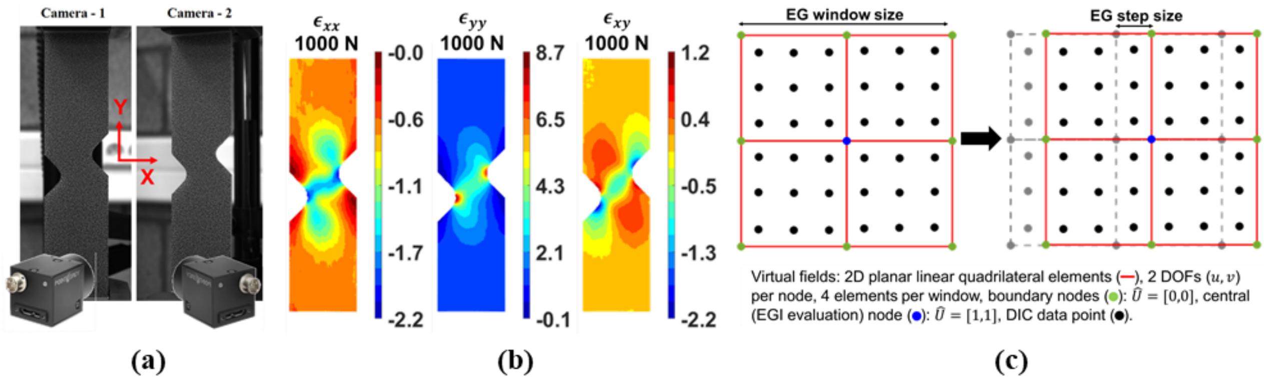

Figure 1: (a) Stereo DIC Setup. (b): DIC strain fields [%] at 1000N load. (c): Equilibrium gap indicator formulation.

To improve hyperelastic material behaviour at small strains, an exponentially decaying linear elastic component is added to the above mentioned hyperelastic material models. The total stress $\boldsymbol{\sigma}^T$ is calculated as:

$$\boldsymbol{\sigma}^T = \boldsymbol{\sigma}^H(\boldsymbol{C}^H, \boldsymbol{\lambda}) + e^{-a\tau}\boldsymbol{\sigma}^L(\boldsymbol{C}^L, \boldsymbol{\epsilon}), \quad \tau = \sqrt{\boldsymbol{\sigma}^{L'}\boldsymbol{\sigma}^{L'}} \qquad \textit{Equation 1}$$

Where H and L stand for hyperelastic and linear elastic contributions, $\boldsymbol{C}^L$ and $\boldsymbol{C}^H$ are respective material parameters, $\boldsymbol{\lambda}$ are the principal stretches, $\boldsymbol{\epsilon}$ are the DIC strains, $\boldsymbol{\sigma}^{L'}$ is the deviatoric part of the linear elastic stress component and τ is the equivalent shear stress.

The equilibrium gap indicator (EGI): EGI evaluates the static admissibility of the full-field stresses calculated using experimental strain fields and an assumed material model. EGI being extremely sensitive to small discrepancies in the stress fields, has been used in the literature to detect damage [2] and material heterogeneity [3] in the context of transverse bending. We adapt it in this work to in-plane membrane situations. EGI window with 4 planar quadrilateral virtual elements is used (refer Figure 1c). The corresponding nodes have 2 degrees of freedom (DOFs): in-plane displacements u and v. This window is moved using a step size to generate a map of EGI and cover the entire DIC spatial domain. EGI is evaluated at the central node, the virtual displacements of which are arbitrarily set to [1, 1]. To cancel the contribution of the material outside the EGI window, the virtual displacements of the boundary nodes are set to [0, 0]. Ideally, EGI should read 0.

$$EGI = \int \boldsymbol{\sigma} : \hat{\boldsymbol{\epsilon}} \; ds = \frac{tS_w}{N_w}\sum_{j=1}^{N_w} \boldsymbol{\sigma} : \hat{\boldsymbol{\epsilon}} = \frac{tS_w}{N_w\overline{\sigma}_w}\sum_{j=1}^{N_w} \boldsymbol{\sigma} : \boldsymbol{B}^*\widehat{\boldsymbol{U}} \qquad \textit{Equation 2}$$

Where $\boldsymbol{\sigma}$ = DIC stress field, $\hat{\boldsymbol{\epsilon}}$ = virtual strain, t = test sample thickness, S_w = EG window area, N_w = # DIC points in EG window, $\boldsymbol{B}^*$ = derivatives of virtual field, $\widehat{\boldsymbol{U}}$ = virtual field.

Reconstructed axial force ratio (RAFR): The axial stress field can be integrated at each cross section along the length of the test sample to reconstruct the force acting at that cross section (refer Equation 3). The actual force applied in the axial direction is known from the tensile test bench. The ratio of the two quantities is termed as reconstructed axial force ratio (RAFR) and should ideally be equal to 1.

$$F_c^i = \int \sigma_{yy}^i \, ds = \frac{t l_i}{N_i} \sum_{j=1}^{N_i} \sigma_{yy}^j , \qquad RAFR^i = \frac{F_c^i}{F_a} \qquad \textit{Equation 3}$$

$\sigma_{yy} =$ axial DIC stress, $t =$ test sample thickness, $N_i =$ number of DIC points along cross section i, $l_i =$ test sample width at cross section i, $F_c^i =$ reconstructed axial force, $F_a =$ actual axial force.

Results: Figure 2 shows the EGI and RAFR at two load levels: 199N (approximately 0.5% peak axial strain i.e., low strain regime) and 998N (approximately 8.7% peak axial strain i.e., moderate strain regime). The EGI in the low strain regime is mostly dominated by DIC measurement noise which is visible as a random pattern. In this regime, linear elastic - hyperelastic material models are superior in terms of the RAFR compared to their pure hyperelastic counterparts. The linear elastic – hyperelastic material models are superior in terms of the EGI at moderately high strain levels. Yeoh material model with the largest number of material constants out of the fitted material models gives the best outcome in terms of the EGI. It is clear from RAFR plots at 998N that none of the fitted material models can accurately capture the material behaviour, especially near the strain concentrations. However, the linear elastic – hyperelastic material models result in flatter RAFR curves meaning in general they tend to outperform the respective purely hyperelastic models.

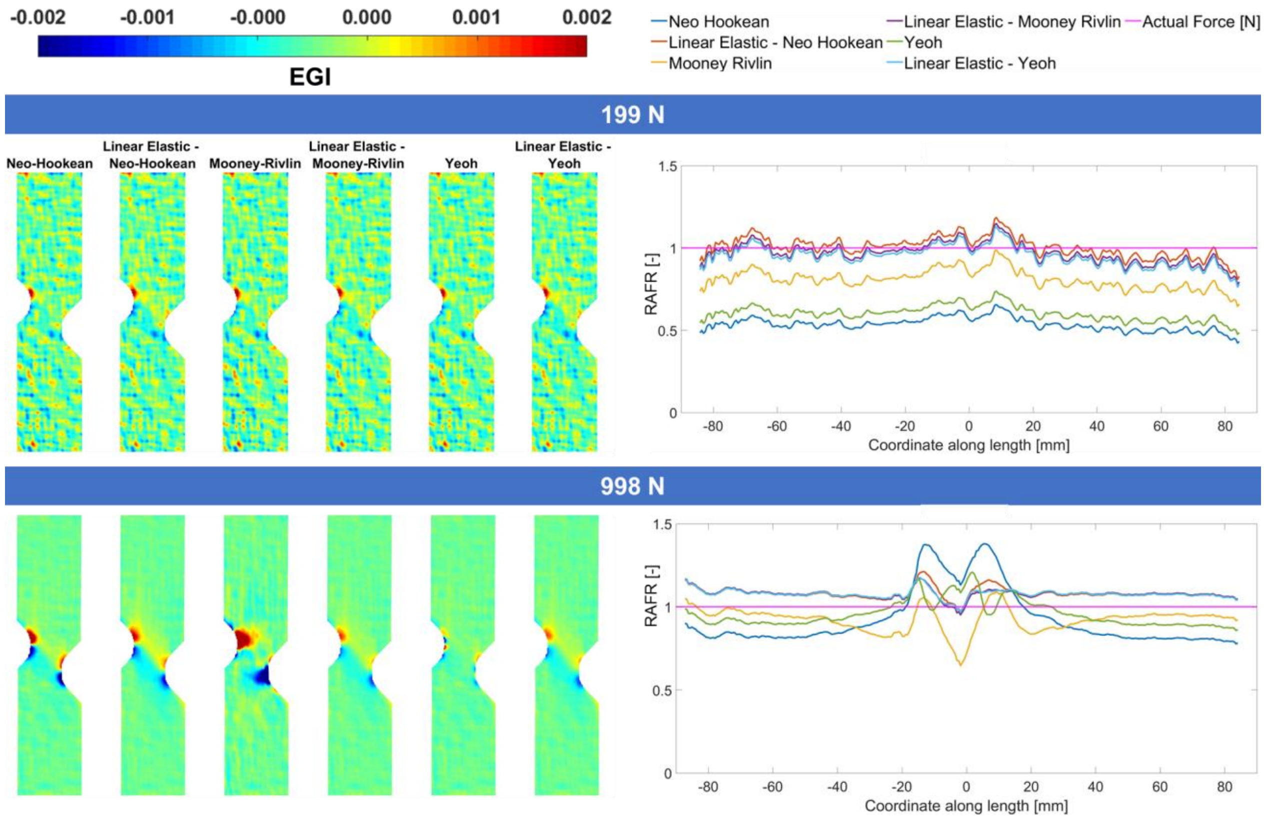

Figure 2: EGI and RAFR at two load levels: 199N (0.5% peak axial strain) and 998N (8.7% peak axial strain).

Conclusions: EGI and RAFR are useful metrics to compare the performance of different material models fitted to the same full-field data in this study. Both the indicators exhibit different information regarding material model performance and are essential. Given the complex nature of polymers, a more advanced material model capable of characterising the viscoelastic and viscoplastic behaviours is necessary to accurately characterise HDPE. This is the future scope for this study.

References

[1] F. Pierron and M. Grédiac, The Virtual Fields Method, Springer, 2012.

[2] C. Devivier, F. Pierron and M. Wisnom, "Impact damage detection in composite plates using deflectometry," *Composites Part A: Applied Science and Manufacturing,* vol. 48, pp. 201-218, 2013.

[3] J. Considine, F. Pierron, K. Turner, P. Lava and X. Tang, "Smoothly varying in-plane stiffness heterogeneity evaluated under uniaxial tensile stress," *Strain,* vol. 53, 2017.